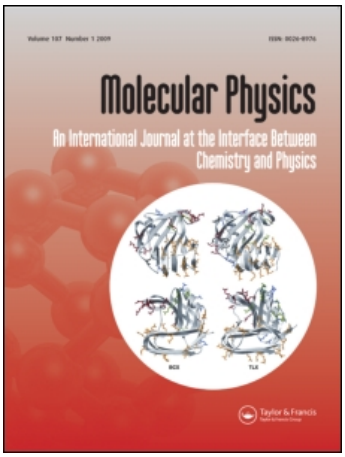

Molecular Physics
Publication details, including instructions for authors and subscription information:
http://www.informaworld.com/smpp/title~content=t713395160

A molecular dynamics simulation: the effect of finite size on the thermal conductivity in a single crystal silicon

Qiheng tang [a]
[a] LNM, Institute of Mechanics, Chinese Academy of Sciences, Beijing, China

Online Publication Date: 20 September 2004

To cite this Article tang, Qiheng(2004)'A molecular dynamics simulation: the effect of finite size on the thermal conductivity in a single crystal silicon',Molecular Physics,102:18,1959 — 1964
To link to this Article: DOI: 10.1080/00268970412331292777
URL: http://dx.doi.org/10.1080/00268970412331292777

MOLECULAR PHYSICS, 20 SEPTEMBER 2004, VOL. 102, NO. 18, 1959–1964

Taylor & Francis
Taylor & Francis Group

A molecular dynamics simulation: the effect of finite size on the thermal conductivity in a single crystal silicon

QIHENG TANG

LNM, Institute of Mechanics, Chinese Academy of Sciences, Beijing, 100080, China

(*Received 2 March 2004; revised version accepted 29 June 2004*)

Non-equilibrium molecular dynamics (NEMD) simulations are performed to calculate thermal conductivity. The environment-dependent interatomic potential (EDIP) potential on crystal silicon is adopted as a model system. The issues are related to nonlinear response, local thermal equilibrium and statistical averaging. The simulation results by non-equilibrium molecular dynamics show that the calculated thermal conductivity decreases almost linearly as the film thickness reduced at the nanometre scale. The effect of size on the thermal conductivity is also obtained by a theoretic analysis of the kinetic theory and formulas of the heat capacity. The analysis reveals that the contributions of phonon mean free path (MFP) and phonon number in a finite cell to thermal conductivity are very important.

1. Introduction

With the dimensions of electronic and mechanical devices approaching the nanometre scale, a demand for greater scientific understanding of thermal transport at atomic scale has been created. Some experiments and theoretical studies have been performed to predict or measure thermal conductivity of nanowire, thin films and periodic film structures [1–6]. Although current experimental techniques can study heat transfer at small scales, the spatial resolution is larger than 100 nm order [7–10]. Moreover interpretation of experiment results remains difficult because typically the contribution of individual defects, such as impurities, grain boundaries and others, cannot be deconvoluted clearly. Even for an individual grain boundary, Cahill *et al.* [10] pointed out that the interactions of phonons with a single interface still offers significant challenges to both experiments and theory/simulation.

There is an increasing demand to develop a method suitable for measuring thermal conductivity for the design of microelectronic devices. The molecular dynamics simulation (MD) method may provide a promising alternative technique both to calculate thermal conductivity and to understand defect mechanisms. MD now is extensively applied to calculate thermal properties because there is no need for an *a priori* understanding of heat transfer. Many MD simulations have been performed on the heat transfer of different structures, such as liquids [11], solids [12], solid–solid interface [13] and of liquid–solid interface [14, 15]. The thermal conductivity can be calculated either using equilibrium MD (EMD) [16, 17] or non-equilibrium molecular dynamics. EMD simulation, based on the Green–Kubo formulation, use current fluctuations to calculate the thermal conductivity at a constant temperature; NEMD is a direct simulation method to calculate the thermal conductivity from the temperature gradient and heat flux crossing the system. The strength and weakness of these two methods have been discussed by Schelling *et al.* [18].

In the present paper, NEMD is used to study heat transfer in perfect crystal silicon. Section 2 details the simulation method; section 3 shows the results of simulation; section 4 displays the size effect of MD simulation and theoretical analysis; section 5 is the conclusion.

2. Computer simulation

Crystalline silicon is a semiconductor material, extensively used in MEMS and integrated circuits. Heat conduction in semiconductor materials is dominated by phonon transport and the contribution to heat conduction by the electrons is negligible. There are several categories of existing potential models for silicon, including the Tersoff type, the Stillinger–Weber (S-W) two- and three-body potentials [19], and others. The S-W potential has been used to simulate the thermal conductivity by several authors. Building on the Tersoff potential, Justo *et al.* [20] proposed the environment-dependent interatomic potential (EDIP) which can better describe the properties of silicon, such as the melting temperature and the thermal expansion coefficient. Therefore, the EDIP potential is selected to simulate heat transfer in our work.

*Author for correspondence. e-mail: qhtang@lnm.imech.ac.cn

Molecular Physics ISSN 0026–8976 print/ISSN 1362–3028 online © 2004 Taylor & Francis Ltd
http://www.tandf.co.uk/journals
DOI: 10.1080/00268970412331292777

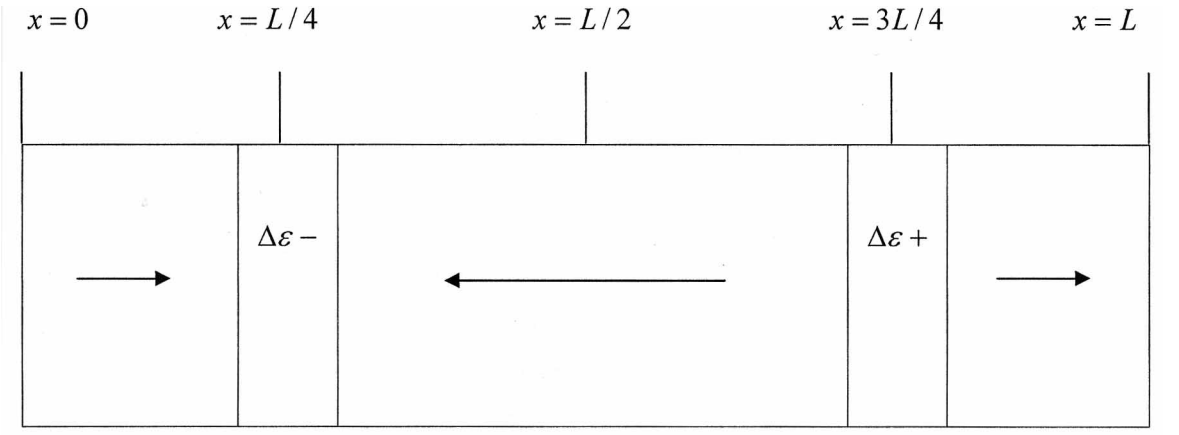

Figure 1. (*a*) Schematic representation of the three-dimensional periodic simulation cell. The simulation cell is parallelepiped with length L_x, L_y and L_z. The heat flow is along the x direction. There is a slab of thickness $\delta = 2a_0$ at $x = L_x/4$ into which energy $\Delta\epsilon$ is removed; likewise, in the slab at $x = 3L_x/4$, energy $\Delta\epsilon$ is added.

Many authors have suggested different simulation techniques to calculate the heat transfer. Some simulation results can be compared to that of experiments or theoretical analyses [21, 22] which activate one's interests of studies and application. Maiti *et al.* [14] studied the heat flow and the Kapitza resistance across a grain boundary. The thermal gradient is applied by maintaining the two end sections at constant but different temperatures. A random thermal wall border condition first proposed by Ciccotti *et al.* [23] can be applied to investigate the heat flow. Jund and Jullien [21] studied the thermal conductivity of vitreous silica, with the techniques of the periodic boundary condition along x, y, z directions and the net kinetic energy increased/decreased by an amount $\Delta\epsilon$ in a thin slab being applied. Based on a similiar NEMD method Schelling *et al.* studied the perfect crystal silicon and compared the result with that of the equilibrium Green–Kubo and found that the results are consistent with each other.

Figure 1 is a schematic of the model system for heat conduction with a three-dimensional periodic simulation cell. A simulation system of parallelepiped cells is selected in this study, and the calculation method for the thermal conductivity κ is analogous to the experimental measurement. The size of the simulation cell is L_x, L_y and L_z respectively. Suppose that the heat transfer is along the x direction and the size in the x direction is larger than that in the other directions. A typical case is that the size for the simulation cell is selected as $44a_0 \times 2a_0 \times 2a_0$, where a_0 is the lattice constant. To calculate the gradient, we divide the simulation cell into j slices along the x direction, the thickness of slice is a crystal constant, $a_0 = 0.543\,\text{nm}$ and there are 32 atoms in a slice in the current simulation. The temperature of particles in the thin slice is calculated at every iteration. According to Maiti *et al.* more than 30 atoms in a slice is needed to yield sufficient scattering events within 1 ns. A simulation with the same number of atoms at every thin slice is given by Schelling *et al.*

The instantaneous temperature in each slice is calculated using the formula

$$(T_{\text{MD}})_j = \left\langle \sum_{i=1}^{N_j} m_i v_i^2 \right\rangle \Big/ 3N_j\kappa_{\text{B}}, \tag{1}$$

where $\langle\rangle$ denotes statistical averaging over all of the simulation time, κ_{B} is the Boltzmann constant, N_j is the atomic number in slice j, $(T_{\text{MD}})_j$ is the temperature in the jth slice, m_i and v_i are the ith atom mass and velocity respectively.

The simulations consist of two stages. The first stage is the constant-temperature simulation, in which the temperature is maintained at constant value using a weak coupling scheme [12] with a coupling time of 200 000 MD steps. At this stage, some authors select a typical run of 50 000 steps; our simulations show that there is no big difference among the final results, the value of the difference being within 3% in this observation. The second stage is the constant-energy one. After equilibrium, a heat flux is imposed on the system along the x direction. A small amount of kinetic energy $\Delta\epsilon$ is added in a thin slab of one crystal constant a_0 thickness centred at $x = 3L_x/4$ and removed from a slab of the same thickness centred at $x = L_x/4$. Our simulations display that the positions of the source/sink can be in any site, but the distance between source and sink should be $L_x/2$ because of the periodic boundary condition. Each particle velocity in the source and sink regions is scaled by the same factor α which is derived from an amount of net kinetic energy $\Delta\epsilon$ increased or decreased.

The energy modification is performed by rescaling the velocities of particles in the source/sink slices. To avoid an artificial drift of the kinetic energy, conservation of the total momentum in the source/sink slices is required. For particle i in the source/sink slice, the scaled velocity [21] is given by

$$v_i' = v_G + \alpha(v_i - v_G), \tag{2}$$

where v_G is the velocity of the centre of mass of the ensemble of particles in the source/sink slice and

$$\alpha = \left(1 + \Delta\epsilon / E_C^{\mathrm{R}}\right)^{1/2} \tag{3}$$

depending on whether the particles are inside the source or the sink slices. The relative kinetic energy E_C^{R} is given by

$$E_C^{\mathrm{R}} = \frac{1}{2}\sum_i m_i v_i^2 - \frac{1}{2}\sum_i m_i v_G^2. \tag{4}$$

By imposing the heat transfer in this manner a constant heat flux J_x can be calculated [21]

$$J_x = \Delta\epsilon/(2L_y L_z \Delta t). \tag{5}$$

The temperature is calculated by equation (1) and the temperature gradient is obtained.

Following Fourier's law used by experiment, the thermal conductivity is determined

$$\kappa = -\frac{J_x}{\partial T/\partial x}, \tag{6}$$

where $\partial T/\partial x$ is the temperature gradient.

3. Results and discussion

A typical time-average temperature profile is presented in figure 2. In this case, the system dimensions are $44a_0 \times 2a_0 \times 2a_0$, and the equilibrium temperature is 500 K. The length $L_x = 44a_0$ is divided into 44 slices. The size of each slice is $1a_0 \times 2a_0 \times 2a_0$, and the local thermal equilibrium is reached within every slice region at 1 ns. Within two lattice constant $2a_0 = 1.086$ nm of the source or sink region, a nonlinear temperature profile is observed, which has been attributed by the strong scattering because of the heat source or heat sink [18, 21].

The data of figure 3 come from that of figure 2. The data are not linear and the fit through the data would change considerably if one or two points on either end were to be excluded. In order to reduce the effect of the high scattering at the heat source and sink, the values of points H and S at the heat or sink source could be justified using the linear extrapolating method. From the values of points C, B and A, we get those of points H and S. The calculated temperature is denoted by open circles and the least-squares linear fits are given for the regions between the heat source and the heat sink regions. From the fitting linear curve, the temperature gradient $\partial T/\partial x$ can be easily calculated. The fits in this case have slopes of (a) $3.60\,\mathrm{K}/a_0$ and (b) $3.66\,\mathrm{K}/a_0$, taking the average. According to the suggestion of Jund and Jullien [21], a suitable $\Delta\epsilon$ may be 1% of $k_{\mathrm{B}}T$; the energy increment $\Delta\epsilon = 0.000\,43$ eV is adopted in our simulations. The heat flux $J_x = 54.188 \times 10^9$ (J m^{-2} s^{-1}) and the thermal conductivity of about 8.1 W mK^{-1} are obtained from equations (5) and (6), respectively.

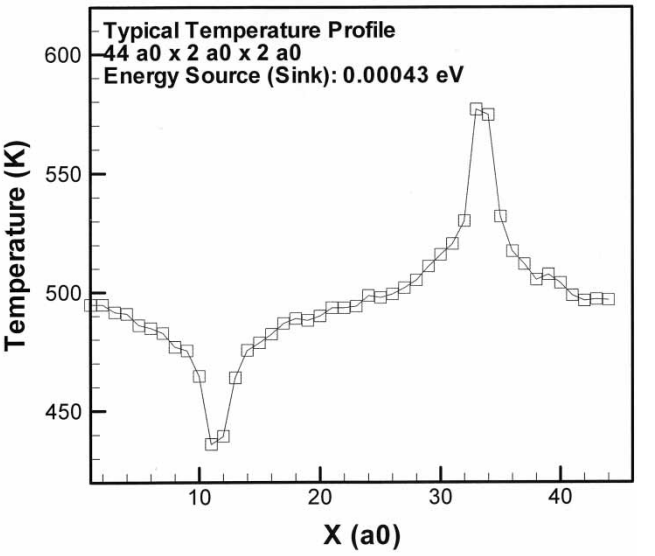

Figure 2. Typical temperature profile for $44a_0 \times 2a_0 \times 2a_0$ at average temperature 500 K. Within $2a_0$ of the source and sink, a nonlinear temperature profile is observed.

It should be noted that the slice j temperature $(T_{\mathrm{MD}})_j$ is obtained from equation (1) which is commonly used in MD simulation; however, it is a classical formula valid only at very high temperature ($T \gg T_{\mathrm{Debye}}$), where $T_{\mathrm{Debye}} = 645$ K is the Debye temperature for silicon. As in this case the system average temperature ($T = 500$ K) is lower than the Debye temperature, it is necessary to apply a quantum correction. Because the system energy from classical statistics should be equal to that from the quantum decription,

$$3N_j k_{\mathrm{B}}(T_{\mathrm{MD}})_j = \int_0^{\omega_D} D_j(\omega) n_j(\omega, T)\hbar\omega\,\mathrm{d}\omega \tag{7}$$

in which $D_j(\omega)$ is the density of states, $n_j(\omega, T)$ is the phonon occupation number, ω is the phonon frequency and $\hbar$ is the Planck constant. From equation (7), we deduce the real system temperature T appearing in the function $n(\omega, T)$. Since the temperature gradient in the Fourier law must also be corrected, the thermal conductivity κ should be rescaled by the $\partial T_{\mathrm{MD}}/\partial T$

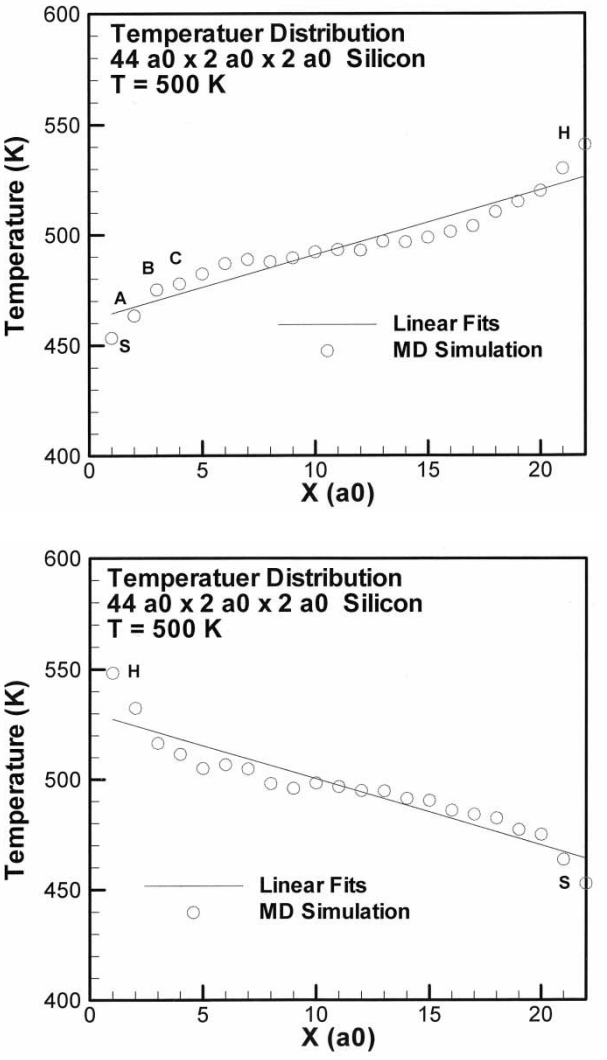

Figure 3. Least-squares linear fits to temperature profiles for the $44a_0 \times 2a_0 \times 2a_0$ system at an average temperature of 500 K. The fits in this case have slopes of (*a*) 3.60 K/a_0 and (*b*) 3.66 K/a_0.

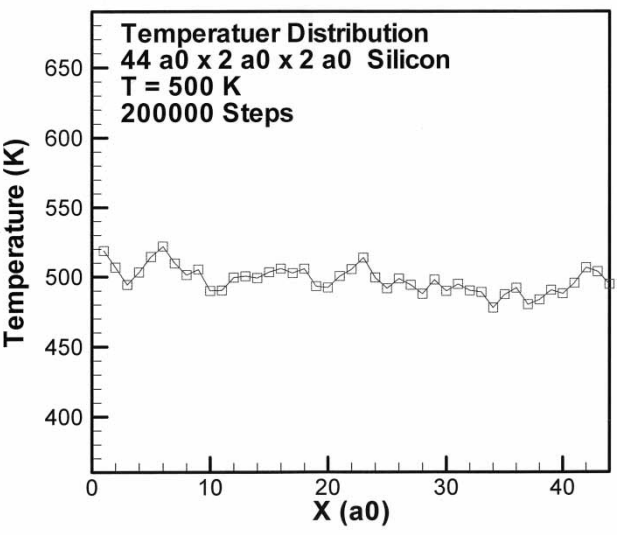

Figure 4. Temperature variation versus space coordinates at the equilibrium state of the system. There is a slight discrepancy for temperature among the slices.

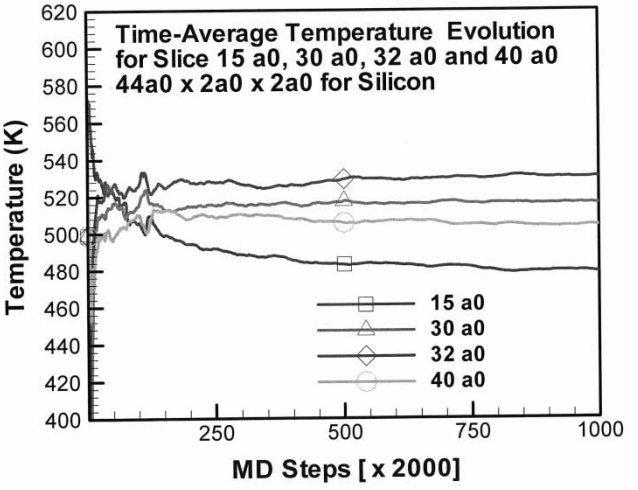

Figure 5. Time evolution of temperature for slices at $15a_0$, $30a_0$, $32a_0$ and $40a_0$ respectively. for $44a_0 \times 2a_0 \times 2a_0$ simulation cell with an equilibrium temperature of 500 K.

factor obtained from equation (7). When the system temperature is 500 K, the correction coefficient $\partial T_{\mathrm{MD}}/\partial T$ is nearly 1. The result given by Volz and Chen [24] shows that the influence of the quantum correction on the thermal conductivity is not significant and our calculations reach the same conclusion.

The temperature evolution versus space coordinates x is shown in figure 4 at 200 000 MD steps, $\Delta t = 0.539 \times 10^{-15}$ s per step. This time, the equilibrium temperature of the system is 500 K, but there is a slight discrepancy among the slices.

Figure 5 shows the evolution of the time-averaged temperature for slice $j = 15a_0$, $j = 30a_0$, $j = 32a_0$ and $j = 40a_0$ respectively. Initially the system is in an unstable state and temperature varies significantly for the first 300 000 MD steps, about 0.17 ns. The system reaches steady state at a time greater than 1000 000 MD steps, about 0.54 ns. This result indicates that 1.08 ns simulation time is long enough to obtain time-averaged temperature profiles, which is in agreement with the results of Maiti *et al.* and Schelling *et al.*

4. Size effect on heat transfer

The results of the size effect on heat transfer have been reported by many authors at the nanometre scale. Schelling *et al.* calculated the thermal conductivity in the NEMD method and displayed the size effects on the

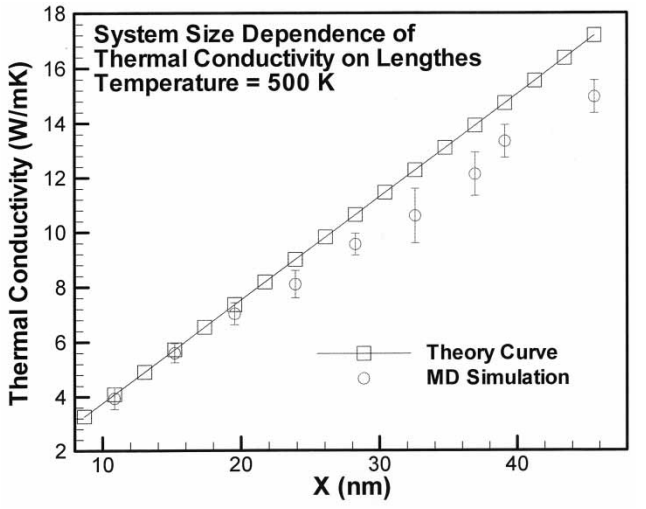

Figure 6. Comparison of the results of the NEMD simulation and theoretical analysis; the size effect on the thermal conductivity is clearly observed.

simulation results. They applied the phonon gas kinetic theory [18]

$$\kappa = \frac{1}{3} C_v v l \tag{8}$$

and the concept of effective MFP l to give an analysis of finite-size effects, and extrapolated it to an infinite system size. Here C_v is the heat capacity per unit volume and v and l are the velocity and mean free path of the phonons, respectively.

Parallelepiped cells are used in the present work. The sizes of the simulation cells are from $20a_0$ to $84a_0$ along the x direction, and $2a_0$ in the y and z directions respectively. There are 9 simulation cells in total. The simulation results are ploted in figure 6; the maximum errors for the simulation results is about 10% which is within the range of the usual estimated value from about 10% to 20% [10]. It is clearly observed that the heat transfer increased with increasing sample size which is in agreement with those of Schelling *et al.* [18] and Feng *et al.* [22].

It is known that the phonon velocity v and MFP are characteristics of the propagative phonons. As for the phonon, there are three polarization modes, the two transverse phonons and a longitudinal phonon which contribute to the thermal conductivity κ in the semiconductor material silicon. The phonon group velocity v varies for the different modes, with $v_{T1} = 5.86 \times 10^3\,\mathrm{m\,s^{-1}}$, $v_{T2} = 2.0 \times 10^3\,\mathrm{m\,s^{-1}}$ and $v_L = 8.48 \times 10^3\,\mathrm{m\,s^{-1}}$. The phonon velocity v in equation (6) is taken as the average phonon group velocity $v_s = 6.4 \times 10^3\,\mathrm{m\,s^{-1}}$ [25, 26]. As for the phonon MFP, there is a great discrepancy among the existing estimation given by Maiti *et al.*, Schelling *et al.* and Yu and Goodson [8]. Compared to the results of Schelling *et al.* and Yu and Goodson, the values of MFP given by Maiti *et al.* are smaller, 20 nm at 1000 K and 30 nm at the Debye temperature. In our simulation, the size of the simulation cell is less than that of the predicated MFP. We can take $L_x/2$, the distance between source and sink regions, as the effective MFP of the phonon [22]. Our simulation box is finite and the number of phonons is also finite, therefore the formula for thermal capacity of a finite system can be applied [21]

$$C_v = \frac{\kappa_B}{V} \sum_p \sum_k \left(\frac{\hbar v_p k / 2k_B T}{\sinh(\hbar v_p k / 2k_B T)} \right)^2, \tag{9}$$

where $V = L_x/2 \times L_y \times L_z$ is the volume, the term $\frac{1}{2}$ is due to the heat transfer direction with the periodic boundary condition. In the expression of C_v the double sum runs over three polarizations $p = L, T1, T2$ and over the first $N/2$ wave vectors, N being the total atom number of the simulation system. The component of the wave vector takes discrete values of the form $k_x = \pm n_x 2\pi / L_x$, where $n_x = 0, 1, 2, \ldots, (N-1)/4$ [27]. From equations (8) and (9), the value of the thermal conductivity for different sizes can be easily calculated.

The theory curve is plotted in figure 6. It shows that the simulation result is in good agreement with that of theory analysis as L_x is less than 28.236 nm. However as L_x is larger than 32.58 nm, deviation is observed and the maximum deviation is about 12%, which is within the numerical simulation error [10]. It is verified that there is a size effect on thermal conductivity, and the NEMD technique is a very good method to calculate thermal conductivity within the nanoscale. When the size of simulation cell is within 24 nm for a perfect silicon crystal, the cell size can be taken as the MFP of a progressive phonon, and the number of phonons is finite. The analysis result implies that the capacity of the finite size cell is different from that of an infinite system.

Applying the method of Schelling *et al.* [18], we can write the following equation:

$$\frac{1}{\kappa} = h_{\mathrm{slope}} \left(\frac{1}{4L_\infty} + \frac{1}{L_x} \right). \tag{10}$$

The curves of equation (10) and the calculated thermal conductivity are plotted in figure 7, where $h_{\mathrm{slope}} = 2.46 \times 10^{-9}\,\mathrm{m^2\,K\,W^{-1}}$ for the EDIP potential, which is a little higher than that of the S-W potential suggested by Schelling *et al.* The benefit of a nice linear fit equation (10) of $1/\kappa$ versus $1/L_x$ is very informative as it allows the true value of the thermal conductivity (the $x \to \infty$) limit to be determined.

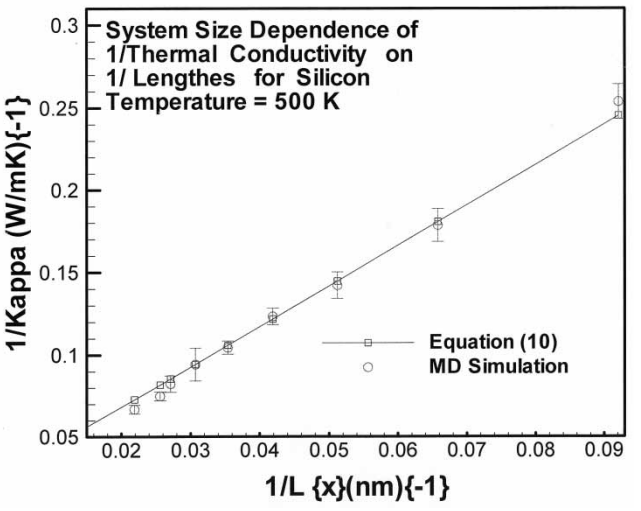

Figure 7. System size dependence of $1/\kappa$ on $1/L_x$. Data are shown for Si at $T = 500\,\mathrm{K}$.

5. Conclusion

The NEMD with periodic boundary conditions is performed with the aim of determining the thermal conductivity in a perfect silicon crystal. The results of the simulation and the theoretical analysis show that the thermal conductivity of nanoscale silicon has a remarkable size effect at a temperature lower than the Debye temperature. In the simulation cell, with a thickness range of 4–40 nm, the thermal conductivity of silicon decreases linearly as the cell thickness is reduced. Our theoretical analysis reveals that the size effect occurs due to following two factors: (1) the effective phonon MFP is greatly reduced when the cell thickness is smaller than that of bulk silicon; (2) the number of phonons which contribute to the heat transfer or thermal capacity is limited when the simulation cell is finite.

The research presented here was supported by the National Natural Science Foundation of China (No. 10342001) and Chinese Academy of Sciences (No. KJCX2-SW-L2), and Institute of Computational Mathematics, Chinese Academy of Sciences (CAS).

References

[1] Cahill, D. G., Goodson, K., and Majumdar, A., 2002, *J. heat Transfer*, **124,** 223.
[2] Li, B., Pottier, L., Roger, J. P., Fournier, D., Watari, K., and Hirao, K., 1999, *J. Eur. ceram. Soc.*, **19,** 1631.
[3] Wang, X., Hu, H., and Xu, X., 2001, *J. heat Transfer*, **123,** 138.
[4] Kulish, V. V., Lage, J. L., Komorov, P. L., and Raad, P. E., 2001, *J. heat Transfer*, **123,** 1133.
[5] Mazumder, S., and Majumdar, A., 2001, *J. heat Transfer*, **123,** 749.
[6] Chantrenne, P., Raynaud, M., Baillis, D., and Barrat, J. L., 2003, *Microscale thermophys. Eng.*, **7,** 117.
[7] Asheghi, M., Touzelbaev, M. N., Goodson, K. E., Leung, Y. K., and Wong, S. S., 1998, *ASME J. heat Transfer*, **120,** 30.
[8] Ju, Y. S., and Goodson, K. E., 1999, *Appl. Phys. Lett.*, **74,** 3005.
[9] Asheghi, A., Leung, Y. K., Wong, S. S., and Goodson, K. E., 1997, *Appl. Phys. Lett.*, **71,** 1798.
[10] Cahill, D. G., Ford, W. K., Goodson, K. E., Mahan, G. D., Majumdar, A., Maris, H. J., Merlin, R., and Phillpot, S. R., 2003, *J. appl. Phys.*, **93,** 793.
[11] Ashurst, W. T., and Hoover, W. G., 1975, *Phys. Rev.* A, **11,** 658.
[12] Floian, M. P., and Simple, A., 1997, *J. chem. Phys.*, **106,** 6082.
[13] Barrat, J. L., and Chiaruttint, F., 2003, *Molec. Phys.*, **101,** 1605.
[14] Maiti, A., Mahan, G. D., and Pantelides, S. T., 1997, *Solid State Commun.*, **102,** 517.
[15] Kincaid, J. M., Li, X., and Hafskjold, B., 1992, *Fluid Phase Equilib.*, **76,** 113.
[16] Volz, S., Saulnier, J. B., and Lallemand, M., 1996, *Physica* B, **219–220,** 476.
[17] Volz, S., and Chen, G., 2000, *Phys. Rev.* B, **61,** 2651.
[18] Schelling, P. K., Phillpot, S. R., and Keblinski, P., 2002, *Phys. Rev.* B, **65,** 144306.
[19] Stillinger, F. H., and Weber, T. A., 1985, *Phys. Rev.* B, **31,** 5262.
[20] Justo, J. F., Bulatov, V. V., and Yip, S., 1998, *Phys. Rev.* B, **58,** 2539.
[21] Jund, P., and Jullien, R., 1999, *Phys. Rev.* B, **59,** 13707.
[22] Feng, X. L., Li, Z. X., and Guo, Z. Y., 2003, *Microscale thermophys. Eng.*, **7,** 153.
[23] Ciccotti, G., Jacucci, G., and McDonald, I. R., 1979, *J. stat. Phys.*, **21,** 22.
[24] Volz, S. G., and Chen, G., 2000, *Phys. Rev.* B, **61,** 2651.
[25] Holland, M. G., 1963, *Phys. Rev.*, **113,** 38.
[26] McConnell, A. D., Uma, S., and Goodson, K. E., 2001, *J. microelectromech. Syst.*, **10,** 360.
[27] Kittel, C., 1971, *Introduction to Solid State Physics* (New York: Wiley).